Design and construction of floating modular photovoltaic system for water reservoirs

Jian Dai[a], Chi Zhang[b], Han Vincent Lim[c], Kok Keng Ang[b,*], Xudong Qian[b],

Johnny Liang Heng Wong[d], Sze Tiong Tan[c], Chien Looi Wang[d]

[a]Department of Marine Technology, Norwegian University of Science and Technology, 7491, Trondheim, Norway
[a]Department of Civil and Environmental Engineering, National University of Singapore, 117576, Singapore
[c]Centre of Excellence for Environmental Sustainability, Housing & Development Board, Singapore
[d]Building & Research Institute, Housing & Development Board, Singapore

Abstract

In May 2018, the Housing & Development Board (HDB) of Singapore piloted the first locally-designed 100 kWp floating photovoltaic system at the world's largest floating photovoltaic cell test-bed in Tengeh Reservoir. This paper presents the various aspects in the development of the floating modular photovoltaic system. This innovative system comprises a number of standardised floating modules made of high density polyethylene (HDPE) that serve as either photovoltaic (PV) panel floaters or maintenance walkways. The structural performance of the floating modules and the inter-modular connectors is assessed through detailed finite element analysis and laboratory tests. The global response of the floating PV system under wave action is investigated by conducting hydroelastic analysis. This paper also presents details of the launching of the proposed floating photovoltaic system at the test-bed and assesses the power generation of the system.

Keywords: floating photovoltaic; renewable energy; water reservoir; finite element analysis; hydro-structural interaction; laboratory test

Kok Keng Ang, Department of Civil and Environmental Engineering,
National University of Singapore, Singapore 117576.
Email: ceeangkk@nus.edu.sg

1. Introduction

Singapore is an island country with only 721.5 square kilometres land area [1]. Although Singapore is land-scarce, the city-state is home to more than 5.8 million people, making its population density the third highest in the world [2]. Like many other mega cities in the world, urban development encounters challenges with regards to availability of useable land space and the ever-growing demand for energy. Due to the lack of natural resources, Singapore has been relying heavily on the import of different fossil fuels to ensure a secure and reliable supply of energy over the past few decades. However, the consumption of fossil fuels has led to environmental concerns. To reduce carbon emissions in the power generation, Singapore started to explore alternative renewable energies to diversify its energy sources and at the same time develop a level of robustness in energy sufficiency. Solar energy was soon recognised as a potential option thanks to the high average annual solar irradiance of about 1663 kWh/m^2 in the region [3]. In recent years, Singapore has been making efforts to accelerate the adoption and integration of solar energy in urban environment. To date, solar energy only contributes to less than 1% of the total energy generation nationwide [4]. There is still a huge opportunity for the use of renewable energy in Singapore.

Despite the high solar irradiance, it is not commercially viable for land-scare Singapore to build large land-based solar farms to generate sufficient solar power. Within densely developed city centres, the urban shading also limits the adoption of solar energy on rooftops. Floating solar photovoltaic (PV) panels on reservoir turns out to be an appealing alternative solution. Floating PV system enjoys several advantages over its land-based counterparts including the natural cooling effect. As reservoir water bodies are located far from tall buildings, structures and vegetation, the receiving of sunlight by the PV panels is thus maximised. Naturally, power generating efficiency is

expected to be higher [5,6]. In addition, the floating PV system provides a cover over the water surface, which substantially reduces evaporation loss of water [7,8]. Furthermore, such shielding effect could also mitigate the undesirable excessive algal growth thus improving the water quality [9].

The benefits of floating PV panels on water bodies soon attracted interests in the energy sector and a number of demonstration and commercial projects have been realised [10,11]. Early designs of floating PV system bear close resemblance to rooftop installations with PV panels typically supported by metallic trusses spanning between polyethylene floaters that are widely used for small floating marinas and piers [12,13]. Presently, the industry is witnessing a growth in the adoption of standardised tailor-made floating modules to house PV panels as well as provide support for operation and maintenance walkways [14-16]. The modular designs permit the size of solar farms to be scalable. Floating modules use less metallic supporting frames as compared to land-based solar farms. Semi-rigid or flexible connectors are often used to connect the floating modules together and to mitigate stress concentration at the connection under wave actions. The allowance for rotation at the inter-modular connection also facilitates the installation and launching of the floating PV farm from a shore ramp to the waterbody. This can greatly shorten the entire construction and installation duration.

Besides the abovementioned designs, many different techniques, design variations and devices have also been introduced to the floating PV system designs. These include submerged PV panels [17,18] which enjoy direct cooling by water, tracking-type PV systems to maximise the collection of solar energy [19,20], and flexible thin film PV panels that yield with rough waves in open sea and offshore conditions [21]. Although various designs have been conceptualised or realised, there is unfortunately very limited

information available in the open literature regarding the design considerations, structural and hydrodynamic performances of the floating system, the manufacturing of floaters, as well as onsite installation and deployment. Such information is not only valuable for researchers and engineers in their analysis and design of floating PV farms but also important for project developers in their evaluation and decision-making.

Recently, Singapore launched the world's largest 1 MWp floating solar PV cell test-bed at Tengeh Reservoir with the aim to investigate the performance of various floating solar energy systems. The field measurement of the power generation and study on the effect of water environment were documented [22]. This paper focuses on the development of a new floating PV system at the test-bed. The innovative floating system is modular in design, formed by connecting tailor-made floating modules of a single shape and size. The floating modules are made of high density polyethylene (HDPE) that serve as either PV panel floaters or maintenance walkways. Detailed finite element analysis is carried out to facilitate the design of the floating module. Hydroelastic analysis is performed for the evaluation of the entire floating system under wave actions. Laboratory testing is conducted to examine the structural capacity of the floating modules. The installation and launching of the floating PV system at the test-bed site as well as the prediction of power generation are also described in the paper.

2. The design

2.1. Design requirements

The new floating PV system installed at the test-bed site is designed for a service life of 25 years. The site is next to an existing floating access bridge which will be used for carrying electrical cables from the floating system to a nearby substation onshore. A shore ramp was also available to facilitate the launching of the floating system onto the

4

reservoir. The key design requirements for the floating PV system are summarised below:

(1) The floating PV system should meet a power generating capacity of 100 kWp.

(2) High density polyethylene (HDPE) material is chosen for the design of the floating modules in view of its material strength and durability in water bodies.

(3) Floating modules shall be able to support 1.65 m long by 1.00 m wide 270 Wp double glass solar panels.

(4) Four inverters need to be supported by floaters next to the PV farm so as to minimise the electricity loss arising from the cable transfer.

(5) A minimum 400 mm wide operation and maintenance access should be provided.

(6) The design of the station-keeping system should cater for an average water depth of 4 m, and up to a maximum of 4.7 m during monsoon seasons.

(7) The design should be cost-effective, lightweight and enable efficient installation and launching of the entire floating system.

In addition, the tilt angle of PV panels should be considered. Since Singapore is located close to the Equator, the optimal all year round fixed tilt is theoretically close to zero degree. However, the local industry advises a 10-degree tilt angle to allow rainwater to wash away the accumulated dust and possible bird droppings from the PV panel surface.

2.2. Structural components

With the abovementioned design requirements, a floating PV system with an overall planar dimension of approximately 60.9 m in length and 23.6 m in width was proposed, as shown in Fig. 1. The floating system is modular in design. Figure 2 illustrates a

typical segment of the system. Dual-pitch configuration of the PV panels is adopted to mitigate the shading effect of one panel to its neighbouring panels. The key structural components include (1) standardised HDPE floating modules, (2) HDPE pillow modules, (3) aluminium PV panel framing units and (4) station-keeping system. In total, there are 888 floating modules, of which 368 floating modules are for supporting PV panels and the rest are used as operation and maintenance access, electrical cable routing and inverter support. Each PV floater is designed to carry one PV panel.

Figure 3 shows the isometric view of a floating module. The module has an overall length of 1260 mm, a width of 400 mm and a height of 215 mm. The module is hollow inside with a thin shell of minimum 3 mm thickness throughout so that it is lightweight (around 6 kg) and buoyant. The top and bottom surfaces are corrugated with ribs and troughs running along the width of the module. These ribs and troughs serve as structural elements stiffening the module surfaces so that the module can carry the imposed loading due to operation and maintenance activities effectively. Furthermore, the corrugation also helps to mitigate possible accidental slipping of maintenance workers. The lower troughs are cambered with a 1-degree slope to prevent stagnation of water to avert mosquito breeding. The standardised modules are equipped with either male or female connecting parts on the four sides so that the modules can be easily interconnected in its longitudinal or transverse directions. The male connecting part comprises a shear key whereas the female connecting part comprises a recess. Connection between neighbouring modules is achieved by fastening the shear key with a stainless steel bolt and nut. The shear keys are designed with rounded corners to mitigate stress concentrations. The connection design aims to provide a stable floating system that can withstand environmental and imposed loadings.

On the module top surface, eight M12 nuts are embedded in the ribs (see Fig. 2). These embedded nuts are utilised when a PV panel is mounted onto the module. The module when loaded with a PV panel is designed to a draft of 100 mm. The same module if used as part of a maintenance walkway is also designed to a draft of 100 mm. By using a single standardised design for the modules, there will be cost-savings as it requires only one type of mould tooling kit. Quality control in the manufacturing of the modules can also be better achieved. The shape and size of the module design is optimized such that the manufacturing can be achieved through either rotational or blow moulding technique.

Figure 4 shows a specially designed pillow structure to support the PV panels. The pillows are made of HDPE with a minimum wall thickness of 3 mm and are designed to be attachable. The attachment to the floating modules is secured by means of bolt and nut connection. The pillow structure elevates the PV panel at one side so that a 10-degree tilt is obtained. As explained earlier, the tilt is needed to allow rainwater to wash off dust and bird droppings in order to maintain efficiency of PV panels.

Standard aluminium back frames and clamps are needed for the fitting of the PV panels and transfer of wind loads to the floating modules. The frames are fastened onto the floater module by bolting to the embedded nuts.

An important component of the floating PV system is the station-keeping system. It has to be designed carefully to prevent the floating PV system from drifting away under adverse environmental conditions. In view of the calm water condition in reservoir and low wind speeds in Singapore, concrete sinkers are used as deadweight anchors. These sinkers are distributed along the length of the floating PV system. A total of 8 concrete blocks, each weighing 4 ton, is designed to resist the drifting force exerted on the floating PV system. Durable nylon ropes are used to tie the floating system to these

concrete sinkers. The variation of water depths (see Section 2.1) has also been taken into account when designing the station-keeping system. The maximum horizontal movement is estimated to be 1 m along both the longitudinal and transverse directions of the floating PV system.

3. Numerical analysis

The performance and design adequacy of the structural components are examined with the aid of numerical simulation tools. The analyses and design checks include two key components, namely (1) the static analysis of the floater module and (2) hydroelastic response of the entire floating system under wave actions from possible different directions. Note that the analysis and design checks of the pillow module and PV panel frames were also carried out but omitted in the paper due to page constraint.

3.1. Static analysis of floating module

The floating module is the key structural component of the floating PV system. The design of the module needs to satisfy the stability, buoyancy, strength and serviceability requirements. As the module is standardized for two intended purposes, two cases of load combinations need to be considered. When the module is used as a PV floater, the key loads acting on the module include the hydrostatic buoyancy force, total dead load including weight of PV panel, framing and mounting accessories, and imposed loads including wind and inter-modular connection loads. When the module is used as a walkway floater, the loads acting are the same except that the dead load comprises only the self-weight of the module. In addition, the imposed loads shall include operation and maintenance loads arising mainly from the weight of a maintenance personnel and equipment carried. For the evaluation of the stress and deformation developed under

8

various load combinations, the finite element method is employed. Figure 5 shows an example of the finite element model of a floating module. The three-dimensional model of floating module is constructed using shell elements. The key inputs for HDPE material properties are: density ρ = 952 kg/m3, Young's modulus E = 500 MPa and Poisson's ratio υ = 0.4. Area springs with stiffness accounting for the hydrostatic pressure are applied at the bottom surface of the floating module. Various loading scenarios were considered in the analysis. Combinations of actions as per Eurocode requirements were accounted for in the design checks. Analysis results show that both stress and displacement are within the allowable limits.

The moment-rotation behaviour of a typical connection between two floater modules is also investigated. This was carried out using a finite element model of the region surrounding a typical connection between two modules, as shown in Fig. 6. The HDPE module and metallic bolts are discretized with thin shell elements and frame elements, respectively. Nonlinear springs are applied to the connection interface between two connected modules to represent the contact condition at the interface. Various magnitudes of force couple are applied to create moments at the connection and the corresponding rotations induced are obtained through nonlinear finite element analyses. The moment-rotation relationship is plotted in Fig. 7, and as can be seen, the relationship is found to be weakly nonlinear. An equivalent linear rotational stiffness of 3.3 kNm/rad may be adopted. Next, a global finite element model of the entire floating system comprising 888 floaters is created. In view of high computational cost, the 3D floating modules are discretized using two-dimensional Mindlin plate elements of equivalent flexural stiffness. The interconnection between modules are modelled using rotational springs with stiffness derived from the previously obtained moment-rotation relationship. Various load patterns accounting for the possible locations of the

operation and maintenance loads have been considered in the global model to evaluate the hydrostatic behaviour of the entire floating system as well as the inter-modular connection loads. The computed connection loads can then be used in the finite element model of the connection between two modules to examine the strength adequacy of the design. The entire design procedure as described is repeated to optimize as well as to ensure compliance of strength and serviceability requirements of the proposed inter-modular connection.

3.2. Hydroelasstic analysis of floating system

Unlike coastal and offshore environment that are exposed to open and rough seas, the reservoir water condition is generally calm. However, waves due to wind and wakes arising from boat passing by can still develop in reservoirs. These waves usually have a short period below 4-6 sec [23] and they impose hydrodynamic forces on the floating modules. When the floating modules are connected to form the floating system, the flexural rigidity of the entire system becomes weaker as its planar dimensions grow. Therefore, the entire floating system will exhibit elastic deformations similar to a flexible plate subjected to wave actions. Hence, hydroealstic analysis is needed to evaluate the wave induced displacement and stress developed.

In the numerical analysis, the floating system is modelled as interconnected Mindlin plates representing the modules floating on an ideal fluid where the linear potential theory is applicable. The rotational stiffness of the inter-modular connection evaluated using finite element analysis is applied in this model. The hybrid finite element-boundary element (FE-BE) approach [24,25] is employed to solve the coupled fluid-structure interaction (FSI) problem in the frequency domain. Figure 8 shows the hydroelastic displacement amplitude per unit wave amplitude *A* under a 5 sec regular

wave propagating with three different wave headings. The corresponding von Mises stress developed due to the wave action is plotted in Fig. 9. Generally, the edge and corner floating modules experience larger hydrodynamic responses when compared with the inner modules. von Mises stress concentrations are found to develop only on modules located near the two end bays in the longitudinal direction under head sea and beam sea waves. Under an oblique wave, high von Mises stresses are observed to develop in the inner floater modules due to induced torsional effects. Note that the representative significant wave height in Singapore water reservoirs is $H = 0.2$ m (or $A = 0.1$ m) [26]. Under such a benign water wave condition, the hydrodynamic responses are small when compared with other analysis results from operation and maintenance loadings. However, it should be noted that wave action and other design actions could occur at the same time. The superimposed responses have been considered in the design of the floating modules.

4. Manufacturing and laboratory testing of floating modules

The floating modules are manufactured using HDPE material. The unique design of the floater and pillow shape makes it suitable to be manufactured using either rotational moulding [27] or injection blow moulding technique [28]. Rotational moulding is ideal for making hollow articles as the technique ensures the uniform distribution of material over the floater hull. However, blow moulding technique was eventually selected due to the urgency to deliver a large quantity of floaters in a short time frame to ensure the assembly of the floating PV system on time. Tests were performed by the manufacturer to ensure the moulding quality and satisfactory material distribution of the fabricated modules.

4.1. Structural laboratory tests

11

In order to ensure that the structural capacity of the produced floating modules is satisfactory, detailed laboratory tests on floating module samples were conducted. The experimental tests include the structural testing of the following four different cases, with all specimens tested to failure:

(1) a single floating module under a monotonically increasing, concentrated vertical loading applied at the centre of module top surface;

(2) two longitudinally connected floating modules under a monotonically increasing, concentrated vertical loading on top of the inter-modular connection interface;

(3) two longitudinally connected floating modules under a monotonically increasing, concentrated lateral loading on the side surface of the inter-modular connection interface;

(4) male connection part under a monotonically increasing, concentrated tensile loading.

These experimental tests were conducted at the Structural Engineering Laboratory in the National University of Singapore. The testing of the first three cases and the last case was repeated three times and four times, respectively, on different specimens. In total, there are 13 specimens tested. Table 1 lists the loading cases and the corresponding specimens.

Table 1: Specimen label for each corresponding loading case.

Loading case	Specimens tested
1: single module under vertical load	SP1, SP2, SP3
2: connected modules under vertical load	SP4, SP5, SP6
3: connected modules under lateral load	SP7, SP8, SP9
4: male connection part under tensile load	SP10, SP11, SP12, SP13

Figure 10 shows the experimental setup of a simply supported floating module under a vertical point load acting at the centre of the module top surface. A horizontal plate of the size similar to a human foot is inserted between the loading fixture and the

floating module to prevent local indentations near the loading point at large deformations. The testing procedure engages a 50-ton Instron universal testing machine (UTM) to a displacement-controlled load at a constant rate of 1 mm/min, which is in accordance to the recommendation in [29,30]. A linear variable differential transformer (LVDT) is used for the monitoring of the vertical displacement along the load line at the bottom surface of the module.

Figure 11 shows the corresponding load-deflection responses at the mid-span of the floating module measured by the LVDT. Also plotted in this figure are the finite element analysis results up to a loading of 1 kN. As can be seen, the floating modules behave almost elastically for loadings not exceeding 1 kN. This is favourable in view that the design load is below this value. For higher loadings, the floating modules undergo plastic deformations, especially when the loading exceeds 1.5 kN for specimens SP1 and SP3 as well as 2 kN for SP2. The ultimate load carrying capacity is found to be 1.78 kN, 2.36 kN and 1.77 kN for specimens SP1, SP2 and SP3, respectively. It is also observed that the specimens SP1 and SP3 exhibit similar load-deformation responses, while the specimen SP2 demonstrates a higher stiffness and ultimate load carrying capacity. Eventually, all three specimens failed due to severe plastic deformations, as shown in Fig. 12.

The testing setup corresponding to the loading case 2, i.e. two connected floating modules subject to a monotonically increasing, concentrated vertical load applied at the inter-modular connection, is shown in Fig. 13. The same support condition, testing machine and displacement-controlled load rate applied to loading case 1 are adopted. This test aims to examine the rotational stiffness and moment carrying capacity of the inter-modular connection.

Figure 14 shows the load-deflection responses and the corresponding moment-rotation responses of the inter-modular connection under a vertical concentrated load. A linearised rotation stiffness of the connection may be derived based on the experimental results up to a rotation level of 0.05 radian. This is found to be 3.1 kNm/rad, 3.5 kNm/rad and 3.2 kNm/rad for specimens SP4, SP5 and SP6, respectively. These values are in a very good agreement with the 3.3 kNm/rad derived from the non-linear finite element analysis results shown in Fig. 14(b), thereby validating the numerical model constructed for the analysis and design of the floating modules. The ultimate moment bearing capacity of the connection is found to be between 350 Nm and 420 Nm. The local failure near the connection holes characterises the primary failure mechanism, as illustrated in Fig. 15.

The loading case 3 is tested with the same configuration except that the load is applied laterally to the connection, as shown in Fig. 16. The testing results plotted in Fig. 17 show that the specimen SP7 exhibits a weaker resistance to the lateral load when compared with SP8 and SP9. This may be due to a slightly larger initial out-of-plane eccentricity in the test setup for SP7, which escalates under increasing applied load. The moment-rotation relationship of the other two specimens agrees very well with the finite element analysis results up to a rotation of 0.05 radian. As expected, the rotational stiffness and moment bearing capacity of the connection corresponding to a lateral load are higher. Severe plastic deformations near the connection zone are observed, characterising the failure mechanisms of the specimens (see Fig. 18).

The connection parts are critical in holding the connected floating modules in place through tension as well as resisting the mooring forces. Thus, their capacity is also examined experimentally. The tensile load carrying capacity of a male connection part is tested by applying a tensile load through a loading pin while the floating module is

fixed with two clamps, as shown in Fig. 19. The testing procedure engaged the same UTM with a displacement-controlled loading at a rate of 0.5 mm/min.

Among the four specimens tested, only SP10 failed at a load of 9.4 kN when the displacement reached 53 mm while others exhibit an increase in the load resistance as the displacement further increases (see Fig. 20). Severe plastic deformations of the connection parts are observed for SP11 to SP13, as shown in Fig. 21. The large deformations in the connection parts engaged the membrane action in the material, which explains the increased tensile load resistance with the applied displacement. Nevertheless, the tensile capacity of all four specimens is far above the calculated design connection load of 2.4 kN exerted by the mooring lines under most adverse conditions.

Table 2 summarises the stiffness of the floating module and connection under various load cases. Note that the stiffness is derived from a linear regression analysis of the experimental load-deformation data up to the magnitude of the design loads. As a comparison, Table 2 also lists the stiffness derived from the finite element analysis. Generally, the experimental and numerical results match very well with each other, with a marginal difference around 5% and below. However, about one third of the specimens are found to exhibit a stiffness that is above 20% different from the others. Locally uneven distribution of material due to fabrication imperfection and small dislocation in the experiment setup may compose the main causes of such differences. This is further discussed in the next section.

Table 2: Stiffness of floating module and connection.

Stiffness (load case)	Experimental	Numerical	Difference
Module bending stiffness (load case 1)	56.2 kN/m (SP1)	54.3 kN/m	3.4%
	83.2 kN/m (SP2)		34.7%
	57.5 kN/m (SP3)		5.6%
Connection bending stiffness (load case 2)	3.1 kNm/rad (SP4)	3.3 kNm/rad	6.5%
	3.5 kNm/rad (SP5)		5.7%
	3.2 kNm/rad (SP6)		3.1%

15

Connection bending stiffness (load case 3)	10.2 kNm/rad (SP7)	12.6 kNm/rad	23.5%
	12.5 kNm/rad (SP8)		0.8%
	13.1 kNm/rad (SP9)		3.8%
Connector tensile stiffness (load case 4)	316 kN/m (SP10)	-	-
	241 kN/m (SP11)		
	247 kN/m (SP12)		
	254 kN/m (SP13)		

4.2. Uncertainty analysis

Uncertainty analysis is important after experimental studies have been conducted and the results from the laboratory test need inspection. In the laboratory test, there exists many sources of uncertainties, for example, measurement errors, fabrication errors and experiment setup errors. In general, the total uncertainty in the laboratory test can be categorised into (1) systematic and constant bias errors and (2) random and varying precision errors. The uncertainties mainly include the error due to geometrical imperfection and the setup position of the module during the test. Unfortunately, it is difficult and sometimes even impossible to carry out a complete uncertainty analysis [31]. Therefore, only the important sources of uncertainty in the experimental study are summarised and discussed.

To identify the uncertainties, repeating tests were conducted during the structural laboratory tests. The comparison of stiffness of different specimens under the same load case between experimental and numerical results gives a direct insight into the level of uncertainties in the experimental test. The errors among the different specimens in each load case have been summarised in Table 2. In general, good agreements can be found between the specimens for the same load case. The results obtained from the repeat tests in load case 2 show a very minor discrepancy up to 3.4%. However, there exist some larger differences in the results of load case 1, load case 3 and load case 4. The differences are discussed below.

For load case 1, it can be found that the numerical and experimental results of SP1 and SP3 show good consistency. However, the stiffness measured using SP2 shows a significant discrepancy at 34.7%. One major uncertainty which has a significant influence is the geometry of the floating module. Due to fabrication imperfection during the blow moulding process, the surface of floating modules may not be perfectly flat for all specimens. The loading acting on the surface is, however, applied through a flat plate beneath the actuator. This implies that the contact area between the loading plate and the outer surface of the specimen may not be consistent, which could lead to different stress distributions as the applied displacement increases. The presence of a curved outer surface also requires a stringent control on the loading position. A small difference in the loading position or plate position may therefore lead to a different stiffness. Also note that the thickness of the modules, produced using blow moulding technique, is hardly expected to be even everywhere. A local variation in the thickness could also contribute to a difference between the results of repeated tests.

For load case 3, a 23.5% difference between numerical and experimental results has been found. Since the load was applied to the side surface of the specimen, which is a flat plane, such a significant difference could be due to how the load was applied. Furthermore, another possible factor could be due to the tightening of the bolts at the connection between two tested modules. Note that manual tightening, instead of tightening by a machine, was used in the experimental test due to constraints of test conditions.

For load case 4, results from the tests on SP11, SP12 and SP13 are consistent, and the error is within 5.5%. However, the connector tensile stiffness measured using SP10 is 27.76% higher than the mean stiffness of the other three specimens. This error is

suspected to be an outlier. As such, this particular result should be abandoned to avoid the uncertainty which may mislead the conclusion.

The calibration of testing facility and sensors may also lead to different results between the repeated tests. In the structural laboratory test, the load is applied through a 50-ton UTM. A displacement-controlled load at a constant rate of 1 mm/min is applied following the recommendation in [29,30]. The displacement was measured by LVDT. The LVDT was calibrated carefully together with UTM before the laboratory test. So, it is believed that the uncertainty from the testing facility and sensors is minor.

Through the uncertainty analysis, it can be concluded that the test results are of good quality. The structural testing data validated the design of the floating module aided by prior finite element simulations. The experimental tests showed that the floating modules would basically behave linear-elastically under the design actions in a service limit state. Furthermore, all specimens are able to develop plastic deformations, resulting in an ultimate loading carrying capacity of the modules that is larger than the design loads. The manufactured floating modules are therefore found to satisfy the design requirements.

5. Project implementation

The photos in Fig. 22 show how the designed floating PV system was launched. The floating modules were manufactured and delivered to the site in batches together with accessories for modular connection and PV panel support. The floating modules were assembled on the ramp covered embankment in accordance to the global layout. HDPE pillows were then mounted onto floating modules to elevate the PV support frames at one end in order to achieve a 10º inclination angle. The other end of the support frames is designed with a hinge connection. The aluminum frame can be fastened onto the

floating module using bolts and embedded nuts. The hinge connection allows PV panels and support frames to be lifted for ease of installation, maintenance and dismantling.

As the overall dimension of the floating PV system is larger than the size of the ramp, it was impossible to assemble the entire system on the ramp before launching. As such, the assembly and launching of the floating system were carried out in stages. Firstly, a part of the floating system was assembled on the ramp with mounted PV panels. Part of the assembled floating system was then slid down the ramp onto the waterbody, leaving space on the ramp for the assembling of the floating modules and mounting of the PV panels to be continued (see Fig. 22a). This procedure was repeated until the entire floating system was assembled. The inter-modular connection parts are designed with rounded corners and a small gap between the contact surfaces is taken into account for the manufacturing tolerance. These allowed a small rotation at the connection to occur when part of the floating system was on water without inducing undesirable high stress concentration at the connection interface.

In the meantime, buoys for positioning of the concrete sinkers were deployed. Non-GPS surveying equipment was used to position the concrete sinkers. Finally, the assembled floating system was towed to the site location (see Fig. 22b) and moored by concrete sinkers. Electrical cable routing, earthing works, installation of inverters and testing were subsequently carried out on the deployed floating system.

The entire project duration including testing and commissioning is less than 6 months. As the floating system described here has recently been commissioned, the monitoring of performance in energy generation has just started and therefore there is insufficient field data for analysis. However, the annual electricity output E can still be estimated using the formula below:

$$E = A \times r \times Q \times PR \tag{1}$$

where A is the total solar panel area in a PV system installation; r is the PV module efficiency; Q is the annual average solar radiation; and PR is the performance ratio. Given that $A = 600$ m^2, $r = 16.5\%$ [32], $Q = 1663$ kWh/m^2 [3] and with PR set to 80% according to the product manual [32] and relevant field monitoring results [22], this 100 kWp floating PV system installation is able to generate 131.7 MWh of electricity in a year. This could reduce carbon emissions by about 55 tons per annum [33].

The local electricity tariff in recent years is relatively low when compared with the historical data due to the declination in the price of natural gas for electricity generated. However, there is a tendency for the electricity tariff to rise in tandem with the increasing cost of natural gas. This would favour the increase in the net profit of the pilot investment. In addition, an open electricity market programme was very recently launched in Singapore. Opening up the electricity market to competition is expected to bring both challenges and opportunities in harnessing solar energy. On one hand, the electricity rate contestable consumers pay is expected to be lower than the current prevailing electricity tariff. This could further bring down the commercial value of PV installations as the renewable energy is still more expensive when compared with fossil fuels. On the other hand, the government is putting efforts to support the adoption of renewable energy. For example, a digital marketplace for the transaction of renewable energy credits (RECs) has been launched in Singapore to support buyers who are keen to reduce their carbon footprint. The development of the RECs aims to encourage the production of green and sustainable energy, which is in line with Singapore's low carbon targets as part of the Paris COP-21 agreement. RECs would add a monetary value to PV installations. This definitely lends support to the adoption of solar energy.

6. Limitations and applicability

The implementation of the first locally-designed 100 kWp floating photovoltaic system at the world's largest floating photovoltaic cell test-bed in Tengeh Reservoir was a success. It also created awareness and interests among the industry and research in the energy sector, both regionally and internationally. Due to the time and financial constraints, however, the design has limitations that can be further improved in the future. Moreover, the lesson learnt throughout the entire project is also of great value to both engineers and researchers in the energy sector. The main limitations of the design, lessons learnt, solutions and suggested improvements are summarised below:

(1) In the current design, a standardised floating module is used as a PV panel floater or maintenance walkway module. This "one size fits all" design has the advantage of minimising the production cost by eliminating the need for multiple mould tooling kits which is quite substantial for this small-scale pilot project. However, due to the fact that the length of the module is governed by the breadth of a typical PV panel, a sizable gap between adjacent PV panels, as shown in Fig. 23, is inevitable with a 1.65 m long by 1 m wide panel used in this project. Depending on the length of a PV panel to be mounted, this design may not be able to achieve an optimal use of the water space, resulting in a less efficient global layout. The gap may be narrowed by mounting PV panels with longer length. Alternatively, a different size may be designed for the walkway modules such that the gap can be reduced.

(2) An injection hole was created during the blow moulding of the floating modules. The hole was plugged up with sealant at the end of the moulding, but it may pose an area of weakness in the module if the sealing is not done properly. For the first few batches of modules, the hole was left on the side of the modules. It was

21

observed onsite that water seepage occurred for a very small number of modules due to the improperly plugged up holes, resulting in a reduction of the carrying capacity of the modules (see Fig. 24). A temporary solution may be to patch the hole with adhesive material, but it may not last throughout the entire service life. As a remedy, the mould tooling kit was modified to have the injection hole on the top face of the modules. This reduces the potential risk of water seepage. Furthermore, it would be easier for maintenance personnel to pump out the water from top in case there is water seepage into the modules. An alternative solution is to produce the modules using rotational moulding technique.

The design of the floating PV farm was based on the local environmental conditions, as shown in Table 3. However, it is possible to employ the same design in other reservoirs with similar environmental conditions worldwide. Appropriate modifications to strengthen the pillow modules and the connections may be needed for wind speed that is substantially higher than that described in this paper. The water current is usually small in reservoirs. However, if strong current is anticipated elsewhere due to possible water discharge, attention should be paid to the design of station-keeping system and the strength of the connection of tethered modules. A representative wave condition [26] was also considered in the design of the floating PV system. In case of harsher wave conditions, which is rare for water reservoirs, the designer may need to increase the freeboard of floating modules and raise the position of the PV panels to avoid frequent water splashing. Besides water reservoirs, the floating system may also be deployed at shielded coastal locations with similar environmental conditions. In marine conditions, however, the biofouling and corrosion issues need to be accounted for in the modification of the design. For example, additional freeboard of floating modules is needed to accommodate possible marine growth. Alternatively, anti-biofouling paint

or cover could be applied. Metallic parts may be replaced with suitable corrosion resistant materials such as high-strength nylon members to avoid undesirable corrosion in marine condition.

Table 3: Characteristic environmental conditions at Tengeh Reservoir.

Parameter	Value
Fundamental basic wind velocity	20 m/s [34]
Current speed	negligible
Significant wave height	0.2 m [26]
Wave peak period	4 s [26]

7. Conclusions

This paper presents the development of a new floating PV system for use in water reservoirs. The innovative floating system is modular in design, comprising interconnected floating modules. An innovative standardized floating module has been proposed. The modules, made of high density polyethylene (HDPE), can function as either PV panel floating modules or operation and maintenance walkways. The modules are designed with both male and female connector parts which allows ease of interconnection to form a desired global layout. Detailed finite element analysis is carried out as part of the design and optimisation of the floating module. Hydroelastic simulation is performed to investigate the hydro-structural response of the entire floating system under wave actions. Structural testing results of the floating modules are presented. The assembly and launching of the floating PV system at the test-bed are described in detail. The power generation and corresponding reduction of carbon emission are also assessed.

The key features enjoyed by the present design are listed below:

(1) The floating modules are made of HDPE material which ensures a service life of 25 years in water reservoir;

(2) The floating module has a standardised shape and size which allows either rotational moulding or injection blow moulding technique to be used. Only one mould tooling kit is needed for the manufacturing;

(3) The floating module is lightweight and compact in size which is ideal for transportation and storage in large quantities;

(4) A specially designed HDPE pillow can be easily mounted to transform the module into a PV floater;

(5) Detailed structural finite element and hydroelastic analyses of the floating system show that the design adequacy is satisfactory;

Although the floating system is originally designed for use in water reservoirs, the design may be suitable for deployment of floating farms in coastal marine conditions with appropriate adjustments to cater for harsher environmental conditions, biofouling and corrosion issues. The project team is currently working on the development of one of the world's largest floating solar PV system at 5 MWp in coastal marine condition [35]. The experiences gained for the 100 kWp floating PV system in Tengeh Reservoir is invaluable as we seek to overcome the challenges in minimising the wave-induced responses, optimising the mooring design and onsite installation procedure for the larger 5 MWp floating PV farm off the coast of Woodlands.

References

[1] Wikipedia. Geography of Singapore. Retrieved from: https://en.wikipedia.org/wiki/Geography_of_Singapore. [accessed on 27 Sep 2018]
[2] Wikipedia. List of countries by population density. Retrieved from: https://simple.wikipedia.org/wiki/List_of_countries_by_population_density. [accessed on 27 Sep 2018].
[3] Doshi TK, D'Souza NS, Nguyen L, Guan TH, Zahur NB. The economics of Solar PV in Singapore. GSTF Int J Eng Technol 2013;2(1):53-63.
[4] Energy Market Authority. Singapore energy statistics 2018. Retrieved from: https://www.ema.gov.sg/cmsmedia/Publications_and_Statistics/Publications/SES18/Publication_Singapore_Energy_Statistics_2018.pdf. [accessed on 27 Sep 2018].
[5] Tina GM, Rosa-Clot M, Rosa-Clot P. Electrical behaviour and optimization of panels and reflector of a photovoltaic floating plant. In: Proceedings of the 26th European Photovoltaic Solar Energy Conference and Exhibition; 2011. pp. 4371-4375.
[6] K-Water. Groundwork research for commercialization of floated photovoltaic system; 2011.
[7] Ferrer-Gisbert C, Ferran-Gozalvez JJ, Redon-Santafe M, Ferrer-Gisbert P, Sanchez-Romero FJ, Torregrosa-Soler JB. A new photovoltaic floating cover system for water reservoirs. Renew Energy 2013;60:63-70.
[8] Choi Y-K. A study on power generation analysis of floating PV system considering environmental impact. Int J Softw Eng Appl 2014;8(1):75-84.
[9] Alam M, Ohgaki S. Evaluation of UV-radiation and its residual effect for algal growth control. In: Advances in water and wastewater treatment technology. Amsterdam: Elsevier Science B.V.; 2001. pp. 109-117.
[10] Trapani K, Santafe MR. A review of floating photovoltaic installations: 2007-2013. Prog Photovolt: Res Appl 2015;23:524-532.
[11] Sahu A, Yadav N, Sudhakar K. Floating photovoltaic power plant: a review. Renew Sust Energy Rev 2016;66:815-824.
[12] Smyth M, Russel J, Milanowski T. Solar energy in the winemaking industry. Springer, 2011.
[13] Kim S-H, Yoon S-J, Choi W. Design and construction of 1 MW class floating PV generation structural system using FRP members. Energies 2017;10:1142.
[14] Ueda YS, Tsurugi K, Tatebe S, Itoh A, Kurokawa K. Performance analysis of PV systems on the water. In: Proceedings of the 23rd European Photovoltaic Solar Energy Conference; 2008.

[15] Santafe MR, Gisbert PSF, Romero FJS, Soler JBT, Gozalvez JJF, Gisbert CMF. Implementation of a photovoltaic floating cover for irrigation reservoirs. J Clean Prod 2014;66:568-570.

[16] Santafe MR, Soler JBT, Romero FJS, Gisbert PSF, Gozalvez JJF, Gisbert CMF. Theoretical and experimental analysis of a floating photovoltaic cover for water irrigation reservoirs. Energy 2014;67:246-255.

[17] Rosa Clot M, Rosa Clot P, Carrara S. Apparatus and method for generating electricity using photovoltaic panels. WP Patent 2,010,026,542; 2010.

[18] Rosa-Clot M, Rosa-Clot P, Tina GM, Scandura PF. Submerged photovoltaic solar panel: SP2. Renew Energy 2010;35:1862-1865.

[19] Cazzaniga R, Rosa-Clot M, Rosa-Clot P, Tina GM. Floating tracking cooling concentrating (FTCC) systems. In: Conferences Record of the 38th IEEE Photovoltaic Specialists Conference; 2012.

[20] Choi Y-K, Lee N-H, Lee A-K, Kim K-J. A study on major design elements of tracking-type floating photovoltaic systems. Int J Smart Grid Clean Energy 2014;3(1):70-74.

[21] Trapani K, Millar DL. Floating photovoltaic arrays to power the mining industry: a case study for the McFaulds Lake (Ring of Fire). Environ Prog Sustain Energy 2016;35(3):898-905.

[22] Liu H, Krishna V, Leung JL, Reindl T, Zhao L. Field experience and performance analysis of floating PV technologies in the tropics. Prog Photovolt: Res Appl 2018;26:957-967.

[23] Dai J, Wang CM, Ustunomiya T, Duan W. Review of recent research and developments on floating breakwaters. Ocean Eng 2018;158:132-151.

[24] Nguyen HP, Dai J, Wang CM, Ang KK, Luong VH. Reducing hydroelastic responses of pontoon-type VLFS using vertical elastic mooring lines. Mar Struct 2018;59:251-270.

[25] Dai J, Ang KK, Zhang C. Hydroelastic analysis of modular floating barges for hydrocarbon storage facility. In: Randolph M, Doan D, Tang A, Bui M, Dinh V (eds) Proceedings of the 1st Vietnam Symposium on Advances in Offshore Engineering. VSOE 2018. Lecture Notes in Civil Engineering, vol 18. Springer, Singapore.

[26] Wong LH, Tan HS, Wang CL, Lim H, Ho HC, Wang CM, Tay ZY, Gao RP. Floating wetlands at Punggol. IES J Part A: Civil Struct Eng 2013;6(4):249-257.

[27] Crawford RJ, Throne JL. Rotational molding technology. Plastics Design Library William Andrew Publishing: Norwich, New York, 2002.

[28] Kamal MR, Isayev A, Liu S-J. Injection molding. Hanser Publishers: Cincinnati, 2009.

[29] ISO 178: 2010. Plastics – determination of flexural properties. International Organization for Standardization. 2010.

[30] Drummen I. Experimental and numerical investigation of nonlinear wave-induced load effects in containerships considering hydroelasticity. Ph.D. thesis, Norwegian University of Science and Technology, Trondheim, 2008.

[31] ASTM D7264/D7264M-15. Standard test method for flexural properties of polymer matrix composite materials. ASTM International, West Conshohocken, PA, 2015.

[32] Canadian Solar. CS6K- 265|270|275|280 P. Retrieved from: https://www.canadiansolar.com/downloads/datasheets/au/new/Datasheet_CS6K-P_au.pdf. [accessed on 12 Dec 2018].

[33] Energy Market Authority. Electricity grid emissions factors and upstream fugitive methane emission factor. Retrieved from: https://www.ema.gov.sg/statistic.aspx?sta_sid=20140729MPY03nTHx2a1. [accessed on 8 May 2019].

[34] NA to SS EN 1991-1-4:2009. Singapore National Annex to Eurocode 1: Actions on structures. Part 1-4: General actions – Wind actions. Singapore Standards Council, SPRING Singapore: Singapore, 2009.

[35] Sunseap. Sunseap to build one of the world's first and largest sea water floating solar systems. Retrieved from: https://www.sunseap.com/sunseap-to-build-one-of-the-worlds-first-and-largest-sea-water-floating-solar-systems/. [accessed on 12 Dec 2018].
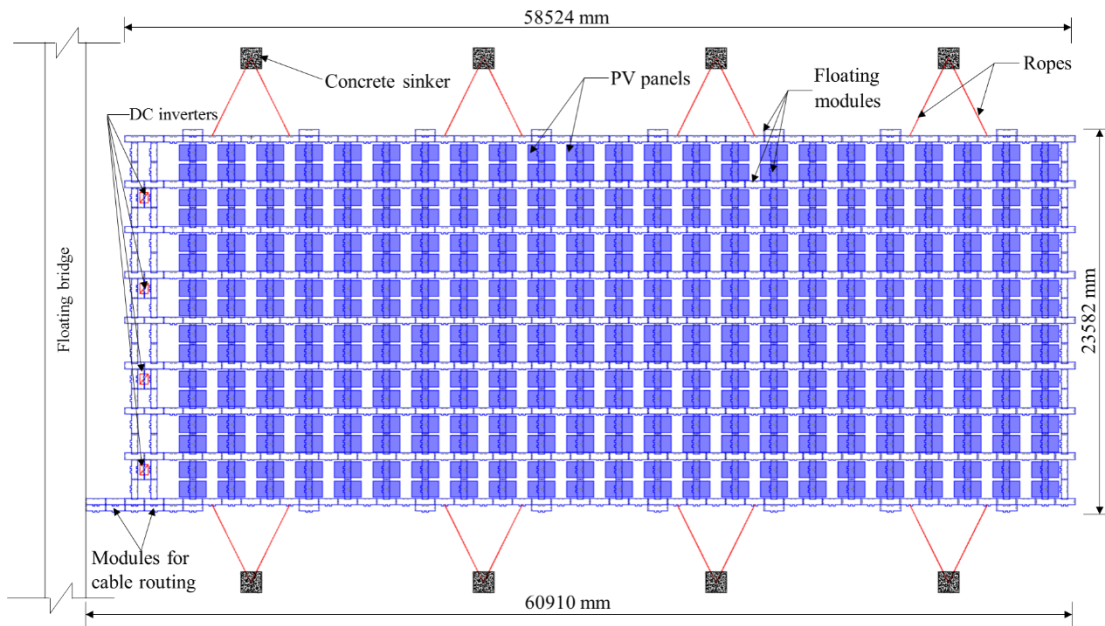
List of figures

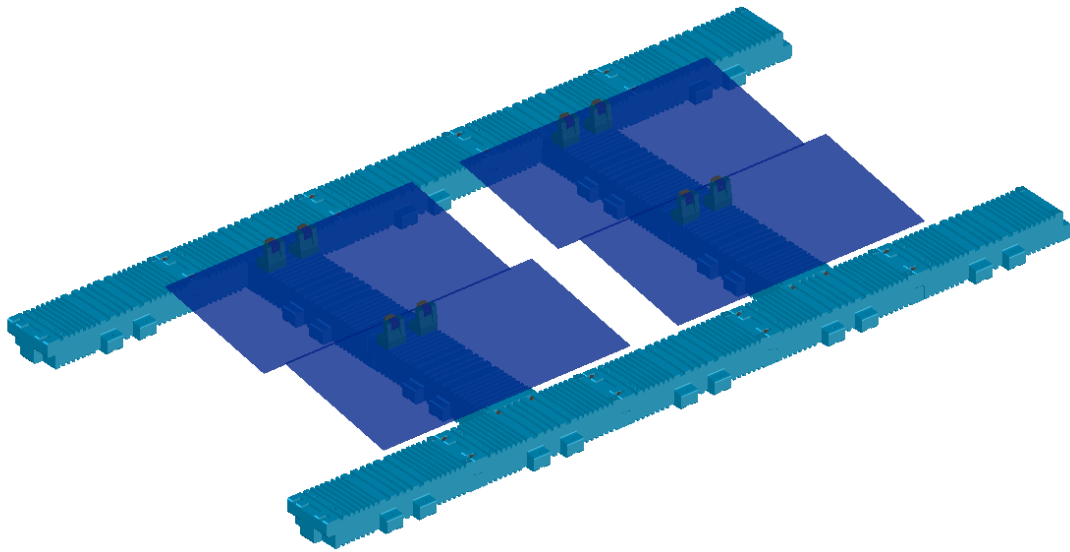Figure 1. Plan view of floating PV system.
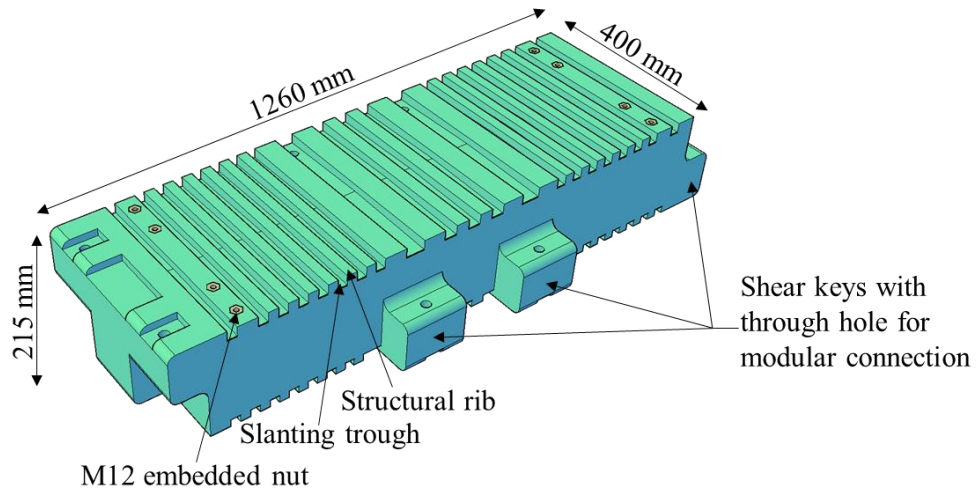
Figure 2. Typical segment of floating system.
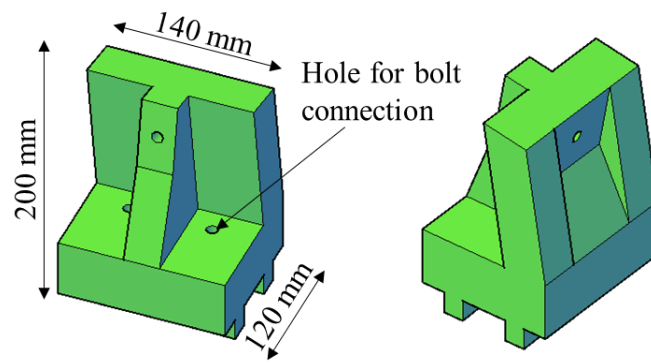
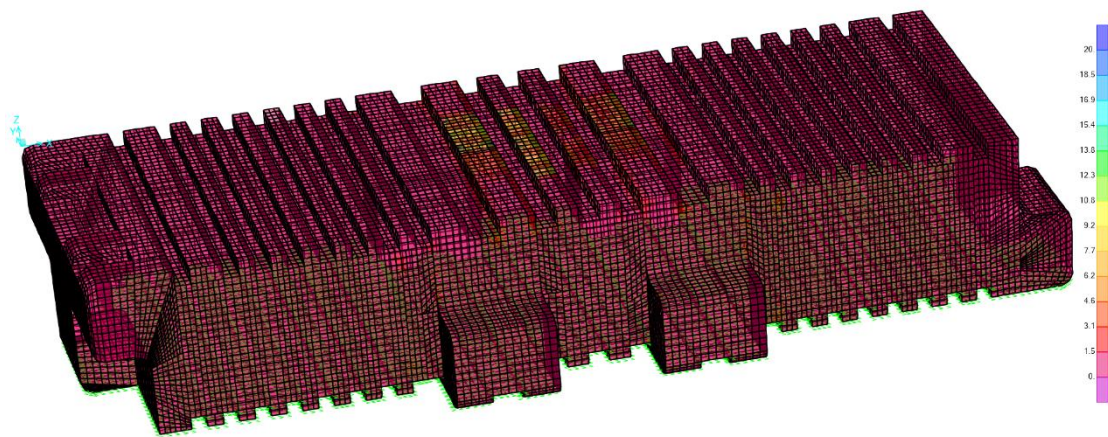Figure 3. Floating module.

Figure 4. Pillow module.

Figure 5. von Mises stress (MPa) contour of floating module under human load imposed at centre of top surface.
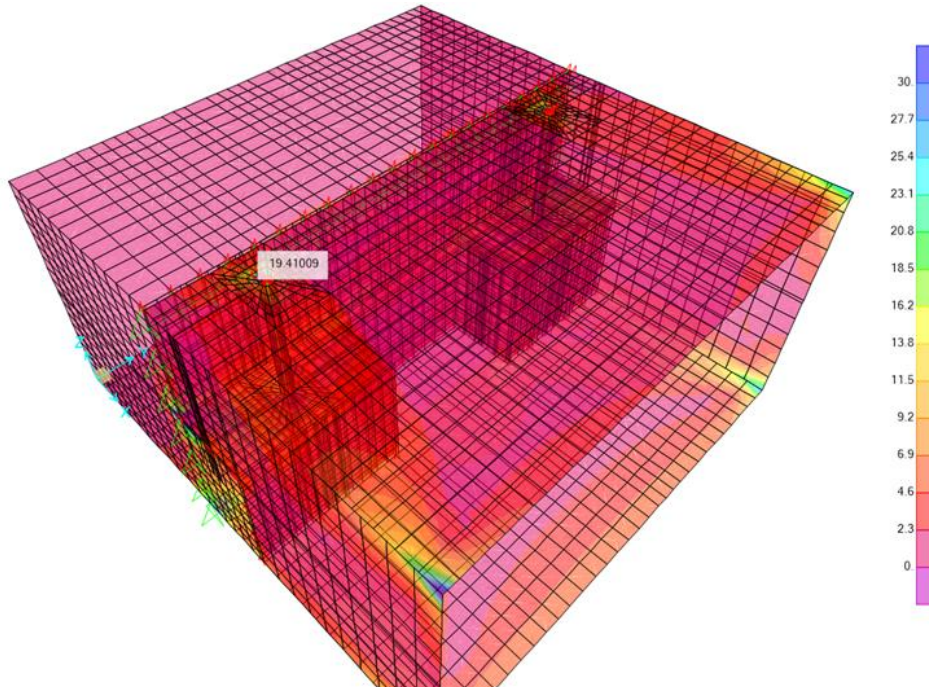
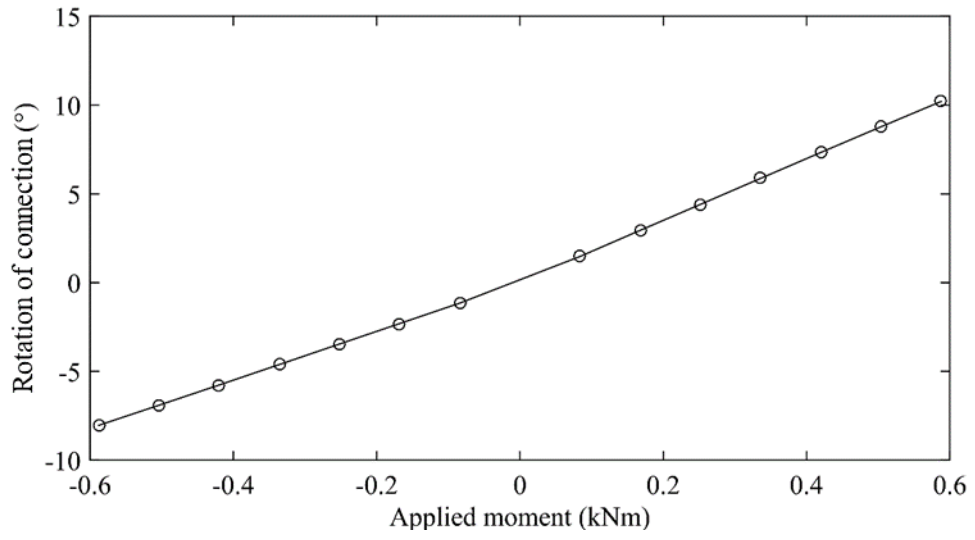Figure 6. von Mises stress (MPa) contour at inter-modular connection.

Figure 7. Moment-rotation relationship of inter-modular connection.

Figure 8. Hydroelastic displacement amplitude (m/m) of floating PV system under 5 sec wave with different headings: (a) head sea wave, (b) beam sea wave and (c) 45° oblique wave.

Figure 9. von Mises stress amplitude (MPa/m) of floating PV system under 5 sec wave with different headings: (a) head sea wave, (b) beam sea wave and (c) 45° oblique wave.

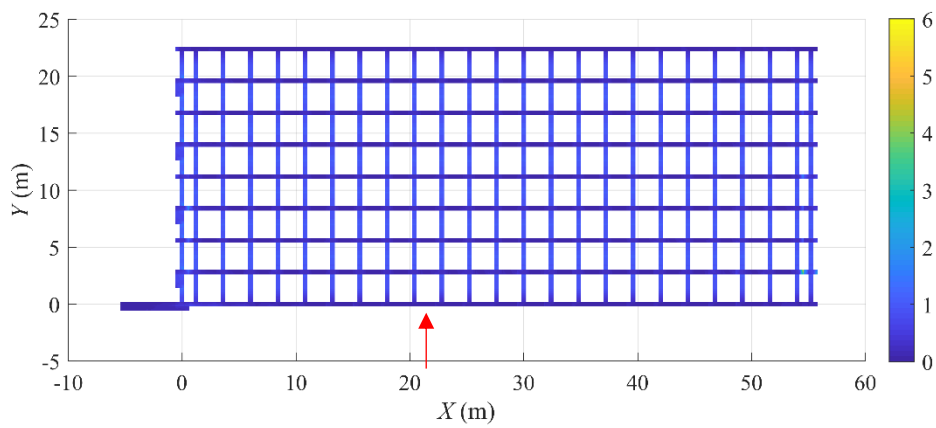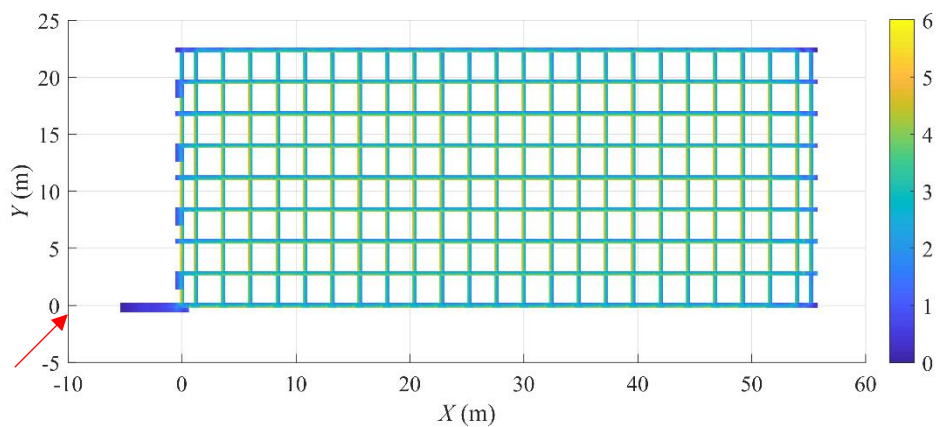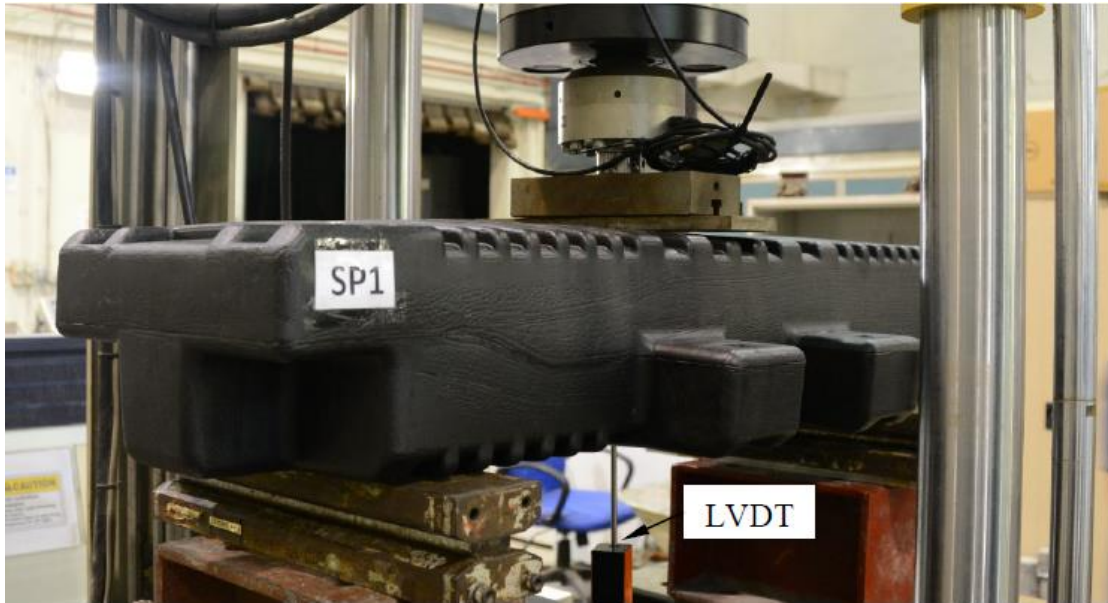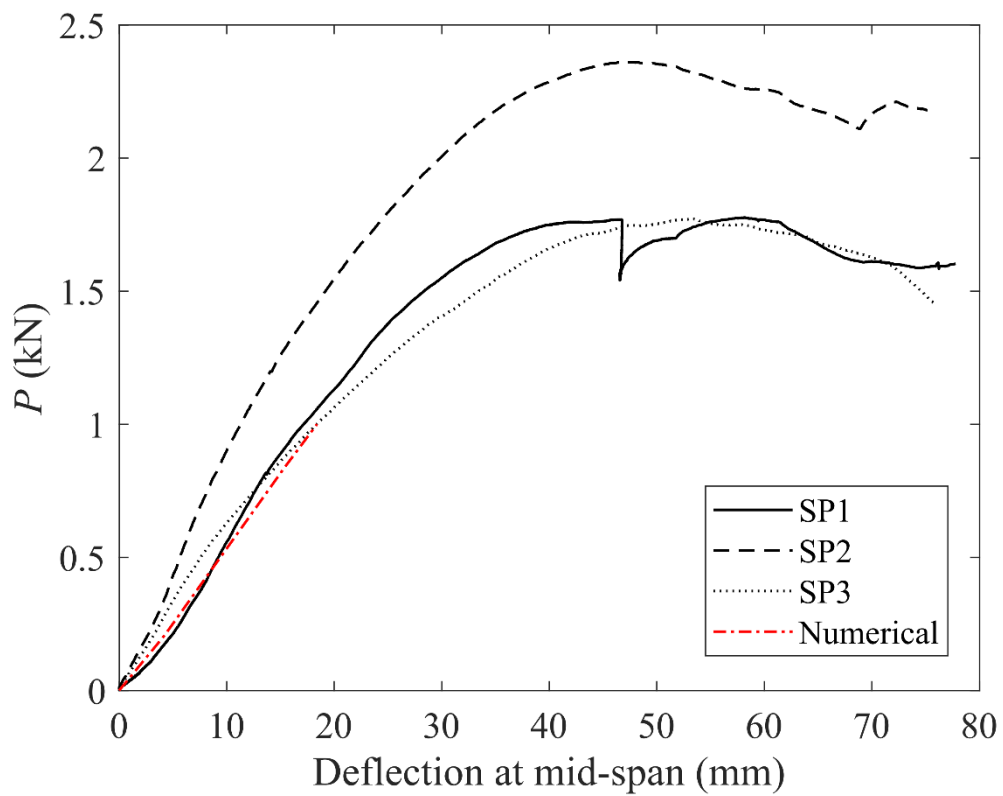Figure 10. Testing setup for loading case 1.

Figure 11. Load versus mid-span deflection for floating module under vertical concentrated loading.

Figure 12. Failure mechanics for floating modules under vertical concentrated load: (a) SP1, (b) SP2 and (c) SP3.

Figure 13. Testing setup for loading case 2.

Figure 14. Experimental results for inter-modular connection under loading case 2: (a) load-deflection responses and (b) moment- rotation responses.

Figure 15. Local failure in or near connection hole: (a) SP4, (b) SP5 and (c) SP6.
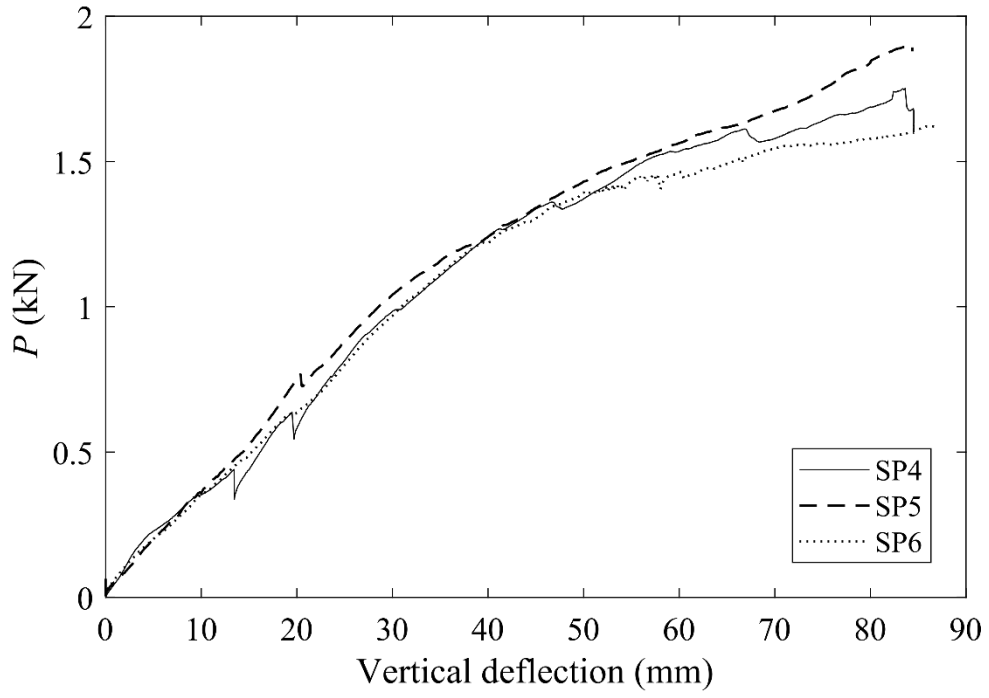
Figure 16. Testing setup for loading case 3.

Figure 17. Experimental results for inter-modular connection under loading case 3: (a) load-deflection responses and (b) moment- rotation responses.

Figure 18. Failure mechanisms for connection: (a) SP4, (b) SP5 and (c) SP6.

Figure 19. Testing setup for loading case 4.

Figure 20. Load-displacement response of male connection part under loading case 4.

Figure 21. Failure mechanisms of male connection part: (a) SP10, (b) SP11, (c) SP12 and (d) SP13.

Figure 22. Launching of floating PV system.

Figure 23. Gap between PV panels.

Figure 24. Unplugged up injection hole on floating module.

Figure 1. Plan view of floating PV system.

Figure 2. Typical segment of floating system.

Figure 3. Floating module.

Figure 4. Pillow module.

Figure 5. von Mises stress (MPa) contour of floating module under human load imposed at

centre of top surface.

Figure 6. von Mises stress (MPa) contour at inter-modular connection.

Figure 7. Moment-rotation relationship of inter-modular connection.
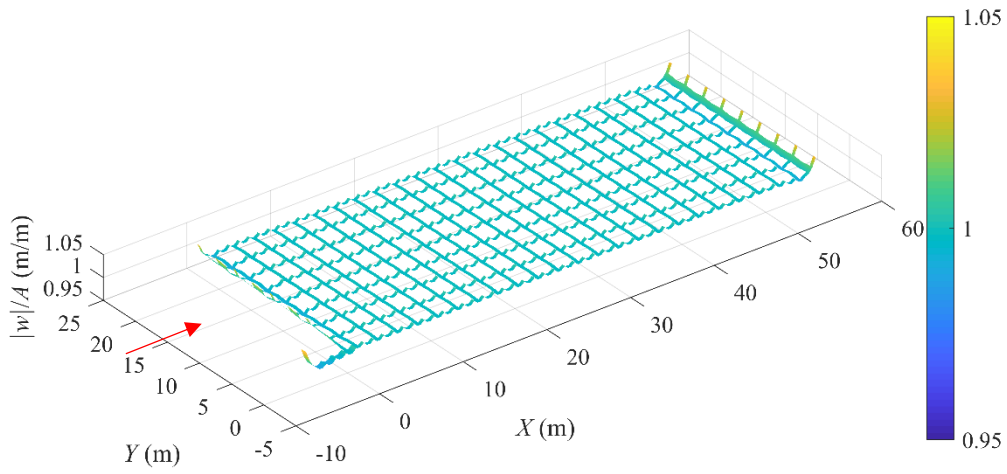
(a)
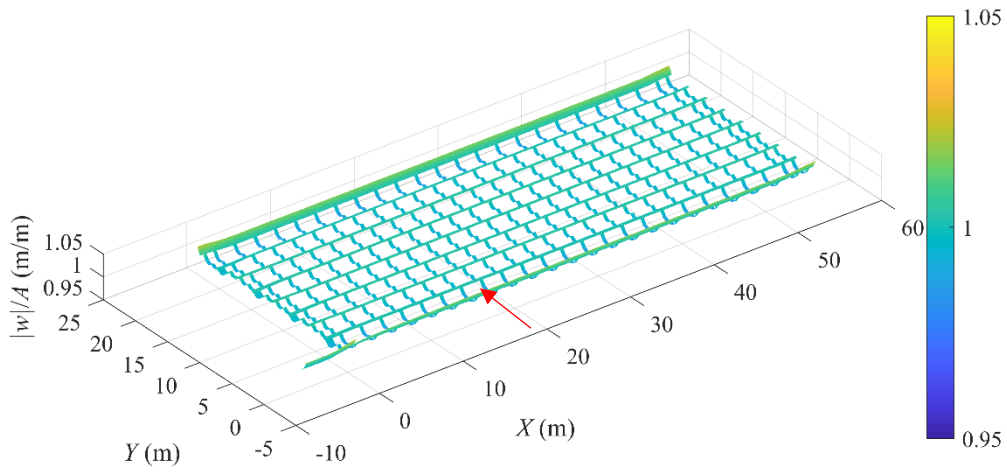
(b)

Figure 8. Hydroelastic displacement amplitude (m/m) of floating PV system under 5 sec wave with different headings: (a) head sea wave, (b) beam sea wave and (c) 45° oblique wave.
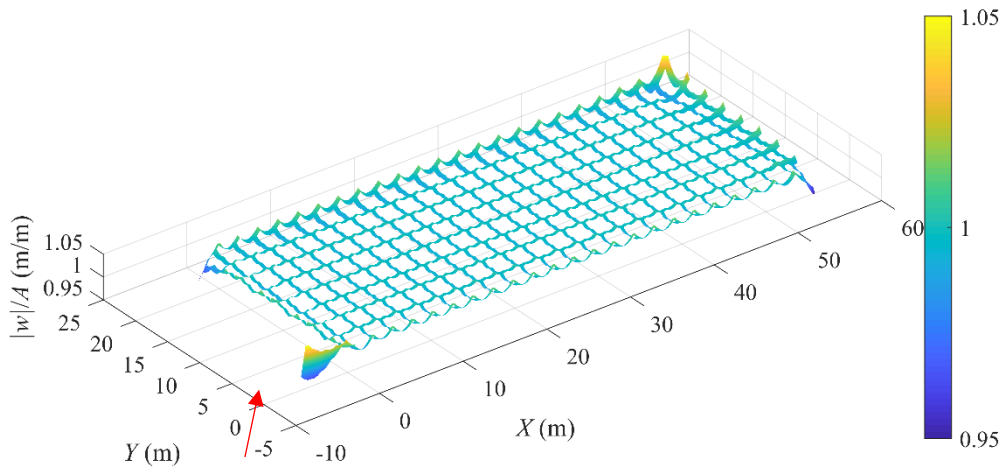
(c)

Figure 8. (*Continued*).
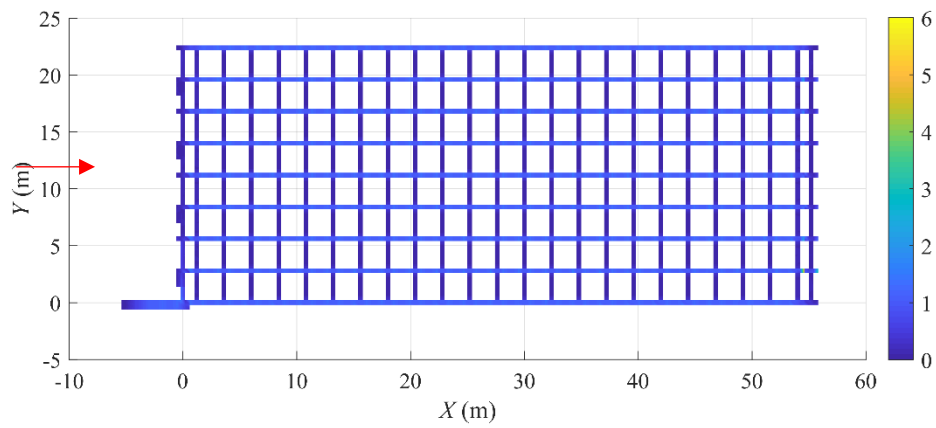
(a)

(b)

(c)

Figure 9. von Mises stress amplitude (MPa/m) of floating PV system under 5 sec wave with different headings: (a) head sea wave, (b) beam sea wave and (c) 45° oblique wave.

Figure 10. Testing setup for loading case 1.

Figure 11. Load versus mid-span deflection for floating module under vertical concentrated

loading.

(a)

(b)

Figure 12. Failure mechanics for floating modules under vertical concentrated load: (a) SP1,
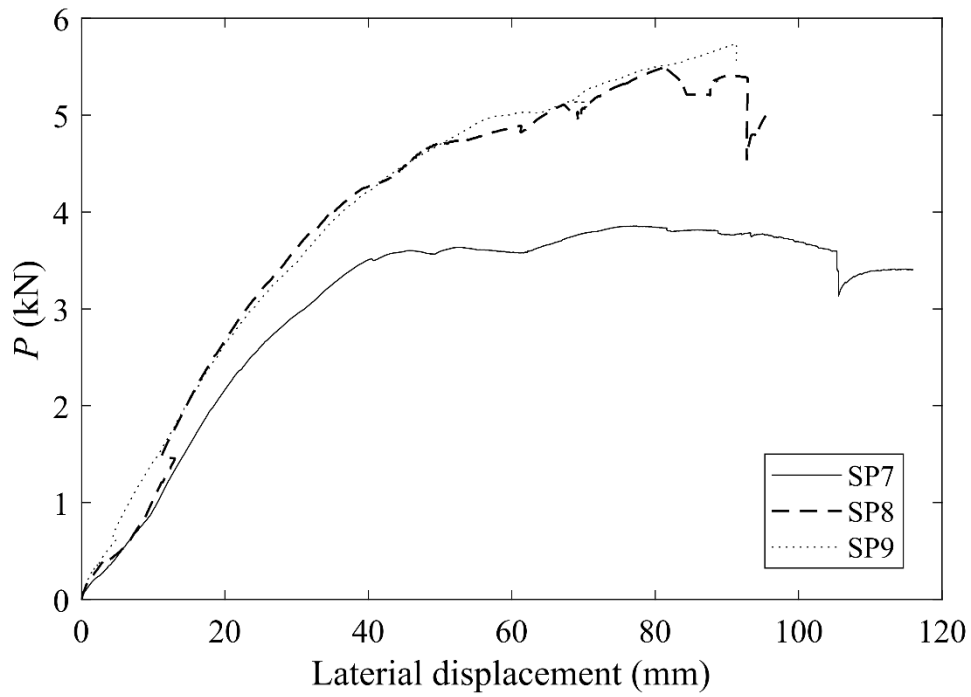
(b) SP2 and (c) SP3.

(c)

Figure 12. (*Continued*).
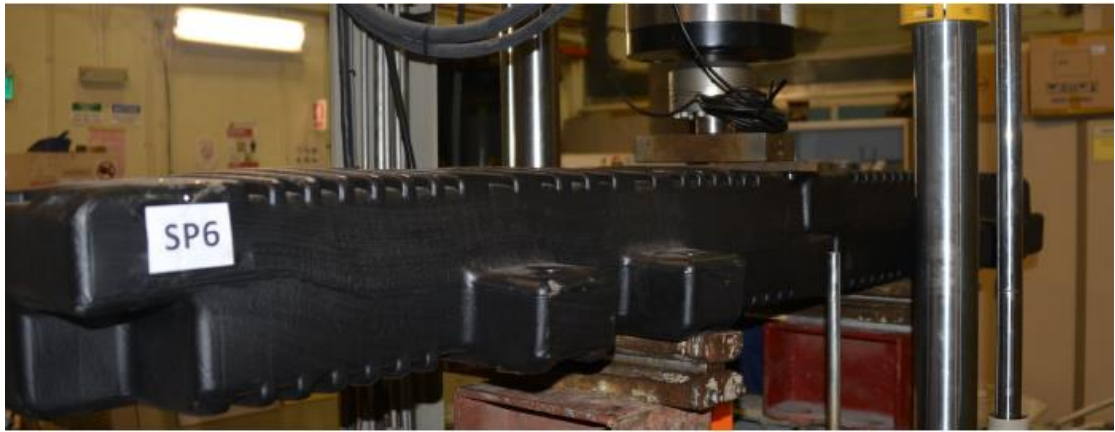
Figure 13. Testing setup for loading case 2.

(a)
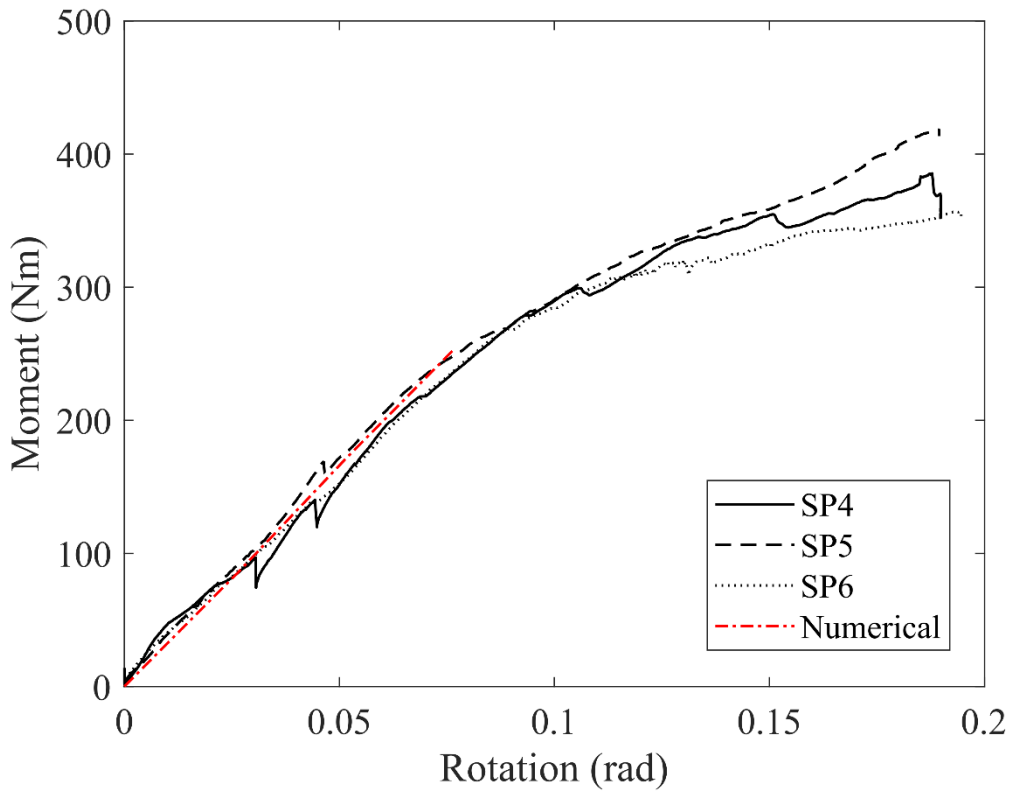
(b)

Figure 14. Experimental results for inter-modular connection under loading case 2: (a) load-

deflection responses and (b) moment- rotation responses.

(a)
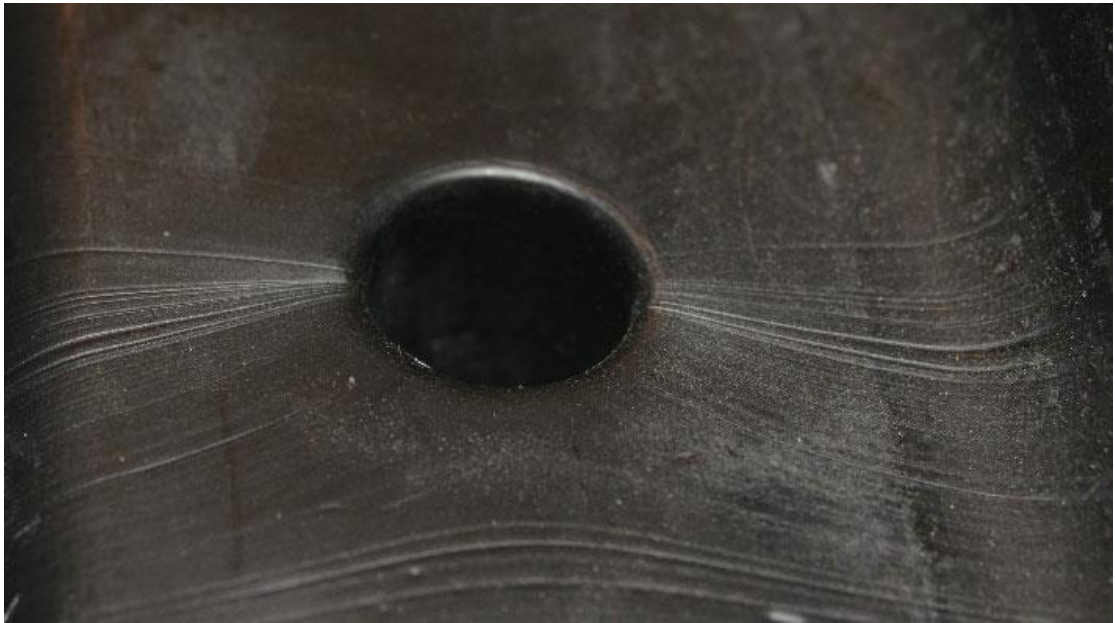
(b)

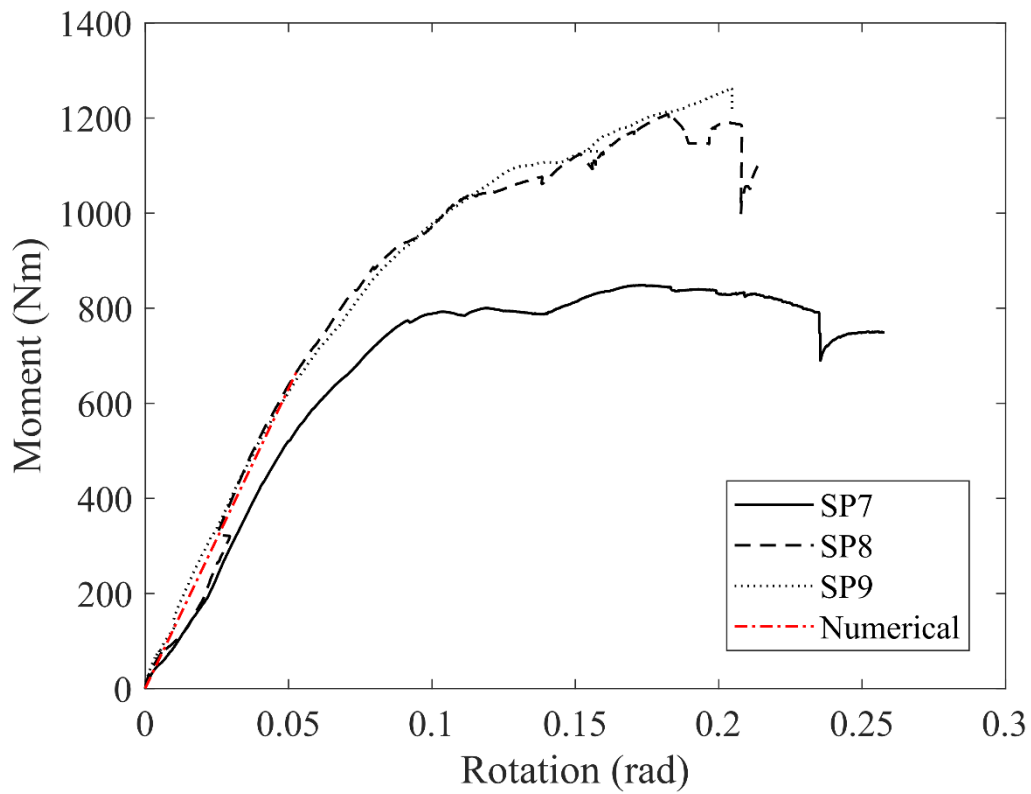Figure 15. Local failure in or near connection hole: (a) SP4, (b) SP5 and (c) SP6.

(c)

Figure 15. (*Continued*).

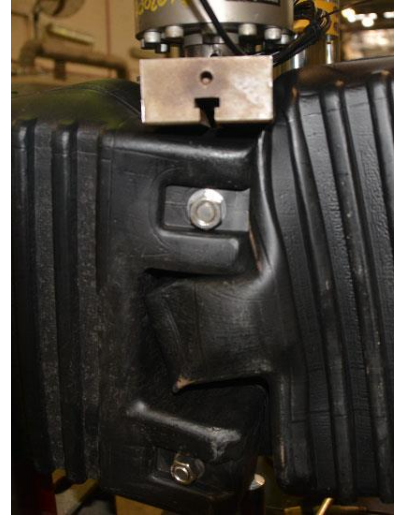Figure 16. Testing setup for loading case 3.

(a)

(b)

Figure 17. Experimental results for inter-modular connection under loading case 3: (a) load-

deflection responses and (b) moment- rotation responses.

Figure 18. Failure mechanisms for connection: (a) SP4, (b) SP5 and (c) SP6.

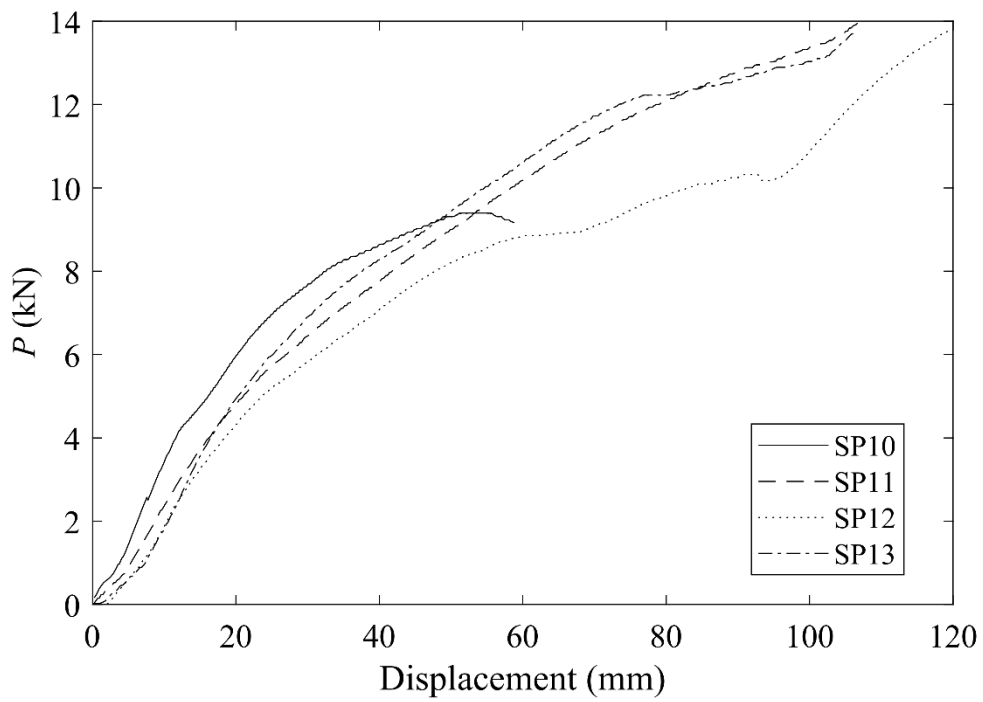Figure 19. Testing setup for loading case 4.

Figure 20. Load-displacement response of male connection part under loading case 4.
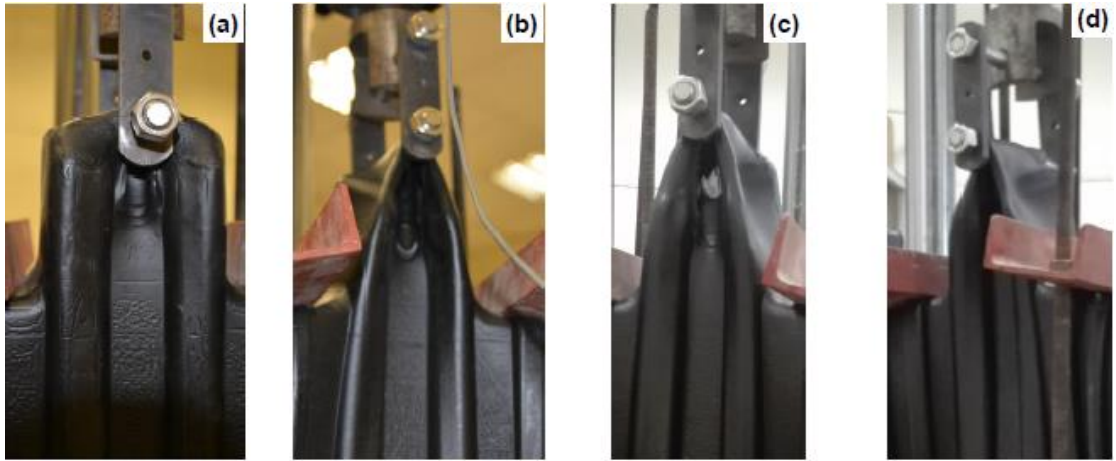
Figure 21. Failure mechanisms of male connection part: (a) SP10, (b) SP11, (c) SP12 and (d) SP13.

(a)

(b)

Figure 22. Installation and launching of floating PV system: (a) assembly on ramp and (b)

deployment on water.

Figure 23. Gap between PV panels.

Figure 24. Unplugged up injection hole on floating module.